STM JOURNALS

Journal of
Materials & Metallurgical Engineering

ISSN: 2231-3818 (Online)
ISSN: 2321-4236 (Print)
Volume 15, Issue 3, 2025
September–December
DOI (Journal): 10.37591/JoMME

https://journals.stmjournals.com/jomme

Research JoMME

Gas Sensors Fabricated Using Carbon Powder Derived from Dried Banana Peels Waste to Detect Methanol, Ethanol, Acetone Vapors and Carbon Dioxide Gas

R.M.A.U. Weerasooriya[1], P.G.D.C.K. Karunarathna[2], P. Samarasekara[3,*]

Abstract

Low cost and environmentally friendly activated carbon powder was synthesized using waste banana peels. Phosphoric acid was utilized as activation agent. Doctor blade method was employed to fabricate films of activated carbon on conductive or nonconductive glass substrates. Films were subsequently annealed at 70°C for 30 minutes in air. According to XRD patterns, single phase of activated carbon was crystallized in thin film form. Carbon prepared from banana peels has never been previously applied to detect methanol, ethanol, acetone vapors or CO_2 gas. The gas sensitivity was measured in 1000 ppm of these vapors or CO_2 gas for 2 hour duration at the room temperature. While the highest gas sensitivity was obtained for acetone vapor, the lowest gas sensitivity was measured for ethanol vapor. Although the resistance of the sample decreased after adsorbing methanol, ethanol or acetone vapor, the resistance of the sample increased after adsorbing CO_2 gas. The optical band gap of carbon films was 4.33 eV as found using UV-visible spectrums. According to SEM images, the particle size was in the range of 2 to 20 μm.

Keywords: activated carbon, banana peels, gas sensitivity, XRD, SEM

INTRODUCTION

Carbon particles derived from biomasses are prime candidates in the applications such as water and purifying, electrodes, super-capacitors, biosensors, catalysis and gas sensors. The biggest challenge in industrial applications is fabrications of low cost carbon powders. The carbon particles prepared from biomasses are one of the best solutions. Carbon particles prepared from pinewood was utilized to remove toxicants such as phenol, 3-chlorophenol, o-cresol, Astrazon Blue FRR, Telon Blue AFN and Methylene blue [1]. Furthermore, carbon particles derived from Mahogany saw dust have been employed to remove toxicants such as direct blue 2B and direct green B [2]. Carbon prepared from Eucalyptus wood was used to remove phenol [3]. In addition, pine saw dust has been applied to remove Malachite Green [4]. Carbon particles fabricated from rubber wood was utilized remove Bismark brown dye [5]. Owing to higher adsorption capacity (2000 mg/g) of rubber wood carbon, they are used in many applications [5]. Hevea Brasiliensis rubber wood saw dust has been employed to detect 1000 ppm of ethanol, methanol, acetone, carbon dioxide, and ammonia gases [6]. Adsorption capacities of carbon particles prepared from pinewood and Fir wood were 1176 and 1476.3 mg/g, respectively [1, 7].

***Author for Correspondence**
P. Samarasekara
E-mail: pubudus@pdn.ac.lk

[1]Research Assistant, Department of Physics, Faculty of Science, University of Peradeniya, Peradeniya, 20400, Sri Lanka
[2]Senior Lecturer, Department of Nano Science Technology, Faculty of Technology, Wayamba University of Sri Lanka, Kuliyapitiya 60200, Sri Lanka
[3]Senior Professor, Department of Physics, Faculty of Science, University of Peradeniya, Peradeniya, 20400, Sri Lanka

Received Date: March 26, 2025
Accepted Date: April 17, 2025
Published Date: September 18, 2025

Citation: R.M.A.U. Weerasooriya, P.G.D.C.K. Karunarathna, P. Samarasekara. Gas Sensors Fabricated Using Carbon Powder Derived from Dried Banana Peels Waste to Detect Methanol, Ethanol, Acetone Vapors and Carbon Dioxide Gas. Journal of Materials & Metallurgical Engineering. 2025; 15(3): 14–25p.

Among biomass derived carbon, some carbon materials provide a higher porosity. The porosity of carbon prepared from Eucalyptus camaldulensis wood is 100% [8]. Different types of activators are used to activate biomass carbon. H_3PO_4 have been used to activate carbon prepared from chestnut wood, cedar wood and walnut wood [9]. $ZnCl_2$ has been utilized to activate Tectona grandis sawdust and pine saw dust [4, 10]. In addition, KOH has been used to activate carbon prepared from Fir wood, Acacia mangium wood and Eucalyptus camaldulensis wood [8, 11, 12]. Carbon fabricated from acacia wood has been widely applied to adsorb toxicants [13, 14]. Carbon prepared from the core and shell of acacia auriculiformis tree branches have been applied as methanol, ethanol, acetone and ammonia vapor sensors [15]. In addition, composites of biomass derived carbon and CuO have been employed to detect 1000 ppm of methanol vapor [16].

Carbon prepared from banana peels find potential applications in various fields. Activated carbon prepared from banana peels have been applied to remove As(III) from water [17]. An ultrasensitive electrochemical sensor has been constructed using banana peel activated carbon/$NiFe_2O_4$ /MnCoFe-LDH nanocomposites for anticancer drug determination [18]. In addition, activated carbon synthesized from banana peels has been employed to remove pharmaceuticals such as amoxicillin and carbamazepine from different water matrices [19]. Banana peel activated carbon has been used to fabricate zinc-ion hybrid super-capacitors [20]. Phosphoric acid has been used for chemical activation of carbon in most of these cases. Banana peel activated carbon has been utilized to remove dye of an aqueous solution in textile industry [21]. Furthermore, banana peel activated carbon has been employed to remove methylene blue in water bodies [22].

In this manuscript, we present the detection of 1000 ppm of methanol, ethanol and acetone vapors using carbon powder fabricated from dried banana peels (Musa genus variety). Comparison of the gas sensitivity in different vapors and gases was the main objective this research. Banana peels were selected to prepare a low cost environmentally friendly gas sensor.

EXPERIMENTAL

Preparation of Activated Carbon Sample

To begin the sample preparation, banana peels (Musa genus variety) were collected and cut into small pieces. After that, they were washed to remove any dirt in the banana peel sample. After washing, the peels were sun dried for five days. Subsequently, the sample was heated in an oven at 105°C until it reached a constant mass. After drying, the sample was crushed into a fine powder. First $ZnCl_2$ acid was tried as the chemical activator, but it was failed. Then, the dried powder was impregnated with 60% concentrated phosphoric acid using an optimized impregnation ratio of 1:1.5 (carbon: phosphoric acid) by weight, and the mixture was soaked overnight to ensure proper absorption of the phosphoric acid into the sample. When there was more phosphoric acid, it was difficult to dry the slurry in the oven to make carbon powder. When there was less phosphoric acid, it was difficult to mix the slurry. Then, 20 g of the sample was heated in an oven at 200°C until it transformed into a black, completely dry residue. Following that, the sample was heated to 500°C for 45 minutes to activate the sample. After the activation process, the carbon sample was thoroughly washed with distilled water and sodium hydroxide in 8 to 10 cycles to remove the residual acid. Finally, the activated carbon sample was dried in an oven at 105°C for 4–5 hours.

Preparation of Films

First, 0.08 g of polyethylene glycol (PEG) was dissolved in 5 ml of distilled water to prepare the binder solution. Then, the PEG solution was stirred at 45°C at 300 rpm for 15 min. After that, 0.42 g of banana peel carbon powder was mixed with prepared PEG solution and stirred at 600 rpm at 60°C until it was suitable to coat on the glass plate. Then, the coating solution was applied on the glass
plate using doctor blade method. After coating, the sample was left to air-dry at room temperature. Following that, the dried sample was heated in an oven at 75°C for 30 min. After that, the sample was

removed from the oven and air-dried. Then, the final 1.5 × 1.5 cm² coated sample was ready for gas sensing applications.

Characterization of the Sample

In this research, the optical properties were determined using UV-Visible spectroscopy. The samples were coated on non-conductive glass plates for the analysis. A Shimadzu 1800 UV-Visble spectrophotometer, operating over a wavelength range of 190 nm to 1100 nm, and it was used to determine the optical band gap of the activated carbon film. The structural properties of the sample were determined using XRD and SEM analyses. For XRD analysis, the samples were coated on non-conductive glass plates, while for SEM analysis, they were coated on conductive glass plates. XRD measurements were conducted using a Rigaku Ultima IV X-ray diffractometer, which utilized Cu-Kα radiation (λ = 1.5406 Å) and scanning over a diffraction angle range from 0° to 100°. The surface structure and particle size of the films were analyzed using SEM (Scanning Electron Microscopy) with a Zeiss EVO LS15 Scanning Electron Microscope, which offers a wide range of magnification capabilities for detailed imaging. Furthermore, a Jandel RM3000+ system was employed to measure the electrical sheet resistance of the carbon films.

Gas Sensitivity Measurement

To measure gas sensitivity, a custom-made chamber with a volume of 76.58 cm³ was used. The experimental setup begins with the connection configured as illustrated in Figure 1 requiring a 5V power supply voltage. In this setup, gold-coated copper wires were employed as electrodes to connect the sample to the circuit. The initial resistance of the sample (R_0) was noted down using a Fluke 289 multimeter. Prior to introducing gas or vapor to the chamber, the circuit was given an hour to stabilize the voltage between the standard resistors. After stabilization, 1000 ppm of the test gas was introduced into the chamber. In this research, methanol, ethanol, carbon dioxide, and acetone were used as the test gases. The voltage across the standard resistor was then measured using a Fluke 28 multimeter over a period of two hours. Gas sensitivity was calculated based on the measurements taken during this two-hour period.

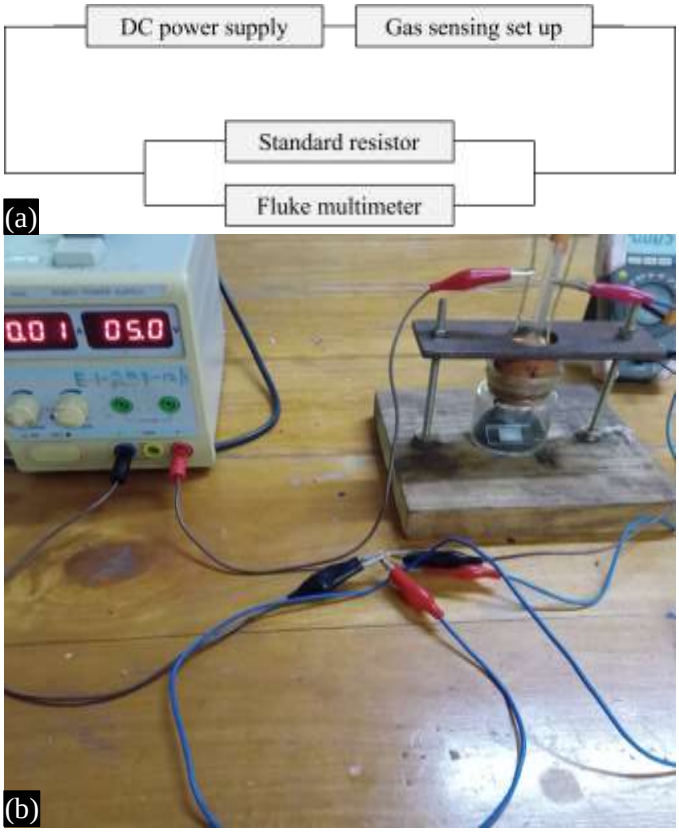

Figure 1. The circuit used to measure the gas sensitivity and an image of the circuit.

RESULTS AND DISCUSSION

XRD Analysis

The XRD pattern was scanned over a 2θ range of 0 to 100 degrees. Peaks corresponding to activated carbon, 7.38°, 23.04°, and 44.50° were observed with Miller indices (001), (200), and (100). This XRD pattern is similar to XRD patterns obtained for activated carbon by some other researchers [23, 24]. According to Figure 2, peak broadening in these samples implies an amorphous nature for the carbon. The width of XRD peaks depends on the amount of activator added in carbon preparation [23]. In addition, the XRD patterns depend on preparation methods such as steam-pyrolysis, standard H_3PO_4 and flowing air [24]. According to XRD patterns, some turbostratic disordered structures have been observed due to the presence of local stacking faults, random shifts between adjacent layers, varying interspacing values, unorganized carbons that are not a part of layer structure, and strain in the layers [23]. Natural lignocellulosic materials consist of various distinct chemical structures, including linear polymeric cellulose, branched hemicellulose, and aromatic, methylated lignin. These components are interconnected and cross-linked through a variety of chemical bonds, resulting in a complex fibrous matrix composite. The crystallite size (D) and strain (□) of the carbon were determined from the XRD pattern of the carbon sample using the Debye-Scherrer equation for crystallite size and the Williamson-Hall equation for strain. The crystallite size (D) and strain (□) of the sample can be calculated using equations (01) and (02).

$$□ = \frac{0.91□}{□□□(□)} \quad (1)$$

$$□ = \frac{□□□□(□)}{4} \quad (2)$$

In this context, λ represents the wavelength of Cu-Kα radiation, which is 1.5406 Å, and β represents the full width at half maximum (FWHM) of the XRD peak measured at an angle θ. In this study, the crystallite size, strain, and dislocation density were calculated for the (002) peak corresponding to a 2θ value of 23.04°. The calculated crystallite size of 1.07 nm for the carbon sample indicates that the material has a very small crystalline domain size. This suggests that the sample has a high surface area, which can influence its physical and chemical properties. A high surface area is particularly beneficial for gas-sensing applications. When considering the strain it depends on mechanical stress, thermal expansion, and defects in the crystalline structure. For the carbon sample, a strain of 3.39×10^{-2} indicates that there is a relatively small deformation in the crystalline structure.

The dislocation density (δ) was determined using the equation (03). In here, the distribution is assumed to be isotropic for dislocations. The calculated dislocation density for carbon sample was 0.87 line per nm^2.

$$□ = \frac{1}{□^2} \quad (3)$$

UV Visible Spectrum Analysis

UV spectroscopy examines how materials absorb ultraviolet light, revealing details about their electronic structure. In the provided graph, three samples with different binders exhibit distinct characteristics in the UV-visible spectrum in the range of 400 nm to 600 nm. Factors affecting the optical band gap include particle size, material composition, crystal structure, and doping. In this study optical band gap of the activated carbon sample was calculated using UV- visible spectrum. The optical band gap of the samples can be calculated using equation (04).

$$E_g = \frac{hc}{\lambda_g} \quad (4)$$

Where, h is plank constant, c is the speed of light, E_g is the optical band gap and λ_g is wavelength corresponding to the optical band gap. The optical band gap energy was calculated as 4.33 eV for an

activated carbon sample synthesized from banana peels. This measured band gap further confirms the formation of activated carbon [25]. Activated carbon usually shows broad absorption across the UV region

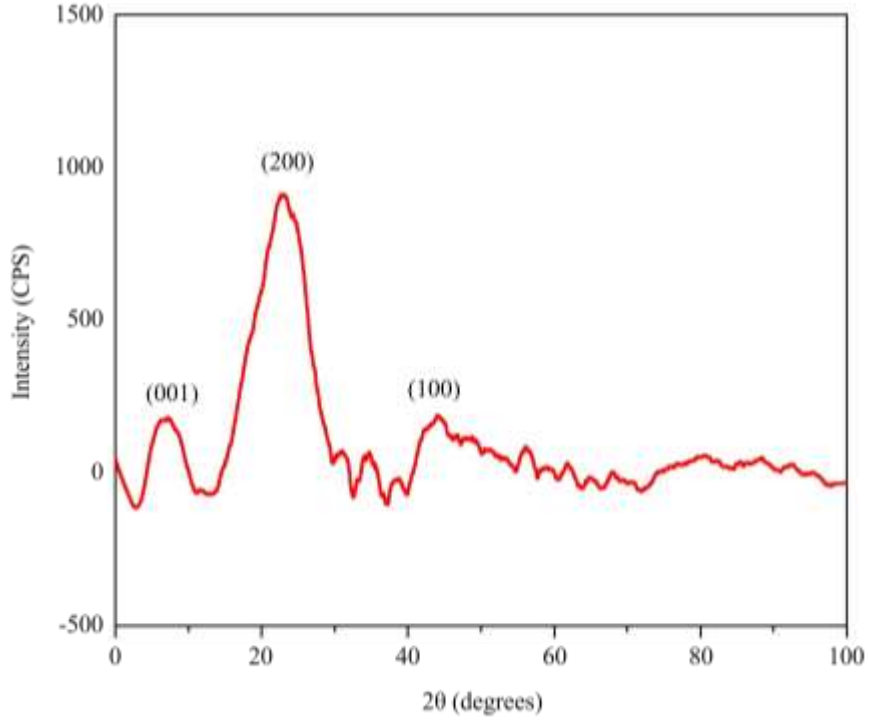

Figure 2. XRD patterns of carbon sample synthesized from the banana peels.

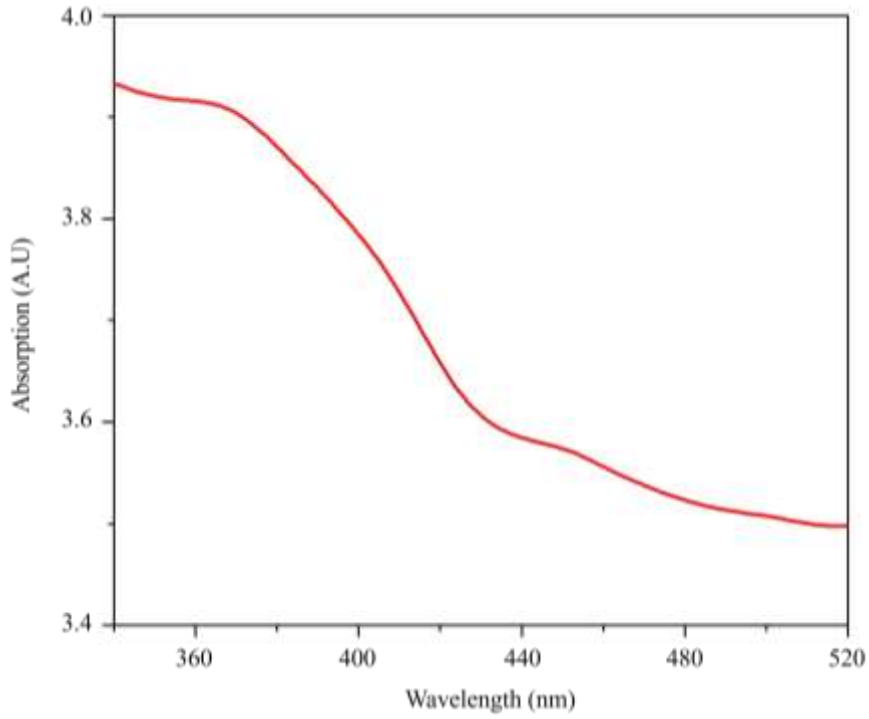

Figure 3. UV-visible absorption spectrum of carbon samples synthesized from banana peels.

and sometimes into the visible range. This is due to the π→π* transitions of conjugated carbon structures (like aromatic rings and graphitic domains) and n→π* transitions from oxygen-containing groups (e.g., carbonyl, carboxyl, hydroxyl). Activated carbon is amorphous or semi-crystalline with a highly heterogeneous structure, so its UV-Vis spectrum generally lacks sharp, well-defined peaks. As the degree of graphitization or conjugated domains increases, the absorption shifts to longer wavelengths (redshift), reflecting more delocalized π-electron systems. In our UV-visible spectrum, absorption has shifted to longer wavelength region. However, the band gap of organic carbon is in the range of 0.35 to 1.7 eV [26].

SEM Analysis

According to the SEM images in Figure 4, the particles exhibit irregular shapes. At a low magnification of 5.00 k ×, the porous structure of the sample is more clearly visible compared to the higher magnification images. When an activated carbon sample has a higher porosity, it enhances the gas adsorption capacity of the sample. Porosity estimated using the ImageJ software was approximately 14%. Porosity of these carbon samples prepared from banana peels is considerably higher than that of carbon prepared from acacia branches and rubber saw dust by us [6, 15]. Particle size varies from 2 to 20 μm.

The particles of carbon samples prepared from some biomasses are in different honeycomb like shapes depending on the activation methods, activation chemical, amount of activator added to carbon, activation temperature and duration [12–14, 27]. The shapes of particles are similar to the particle shape of initial biomass according to these studies. For an example, when the raw acacia wood surface shows partially honeycomb like structure, the particles in carbon sample also exhibit honeycomb like structure. At higher activation temperatures, the pore becomes spherical shapes [12–14]. When the carbon is properly activated, the porosity of the sample enhances. In addition, using the phosphoric acid enhances the porosity compared with potassium hydroxide, calcium oxide, and zinc chloride [12–14]. Furthermore, the porous structure can be improved by increasing the concentration of chemical activator and activation temperature. However, when the activation temperature is increased above a certain limit, the porous structure diminishes [27]. Therefore, our carbon powder samples were heated to 500 °C in the activation process.

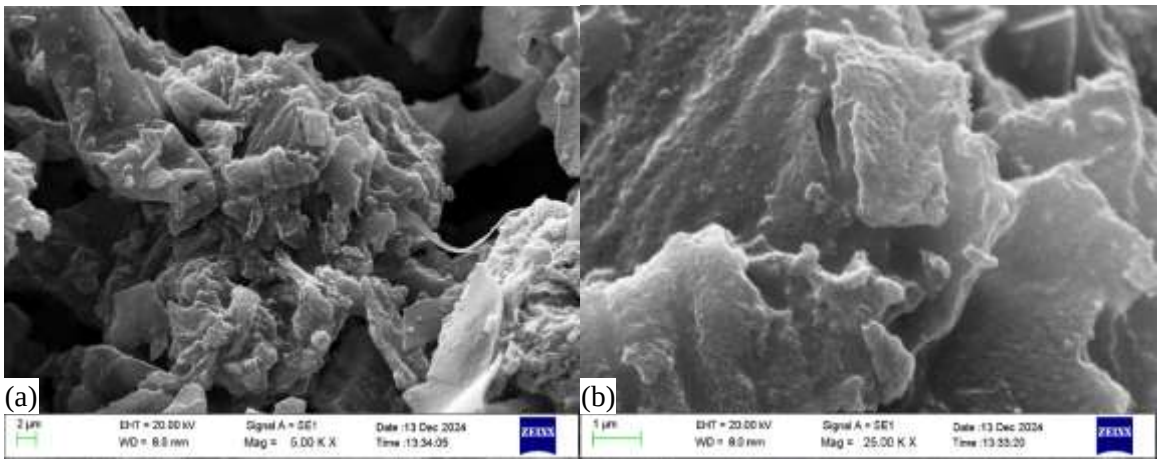

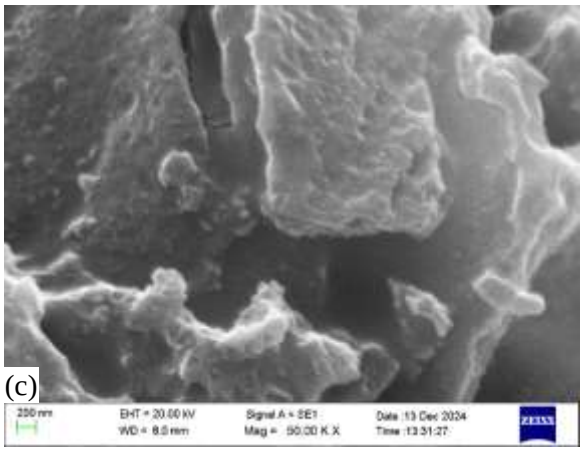

Figure 4. SEM images of carbon films synthesized from the banana peel sample with magnification (a) 5.00 k ×, (b) 25.00 k ×, and (c) 50.00 k ×.

Gas Sensitivity Analysis

In this study, the sample area on the FTO plate was approximately 1.5 cm ×1.5 cm across all samples. To ensure a more suitable comparison, it is important to select a standard resistor that closely matches the resistance of the sample. Gas sensitivity is defined as the percentage change in resistance of thin film in the presence and absence of gas. The gas sensitivity of the sample can be calculated using equation (05).

$$Gas\ sensitivity = \frac{|R_{gas} - R_0|}{R_0} \times 100\% \quad (5)$$

In this study, R_{gas} represents the resistance of the sample after 2 hours upon exposure to the introduced gas, while R_0 is the initial resistance of the sample measured before gas exposure. During the experimental procedure, voltage values were observed across a standard resistor instead of directly measuring the voltage across the sample. This approach was chosen because directly measuring the voltage across the sample is not an effective method, as the resistance of the sample changes continuously upon interaction with the gas until it reaches saturation. V represents the voltage across the standard resistor. The resistance of the sample and the current through the sample were calculated using equations (06) and (07) respectively, based on Ohm's law.

$$\square = \left(\frac{5}{\square} - 1\right) \square \quad (6)$$

$$\square = \left(\frac{5-\square}{\square}\right) \quad (7)$$

Figures 5–7 represent the voltage, resistance, and current responses, respectively, for the activated carbon sample corresponding to methanol, ethanol, carbon dioxide and acetone at a concentration of 1000 ppm. By analyzing these variations over time, the sample can be evaluated for suitable applications.

According to Figure 5, after introducing test gases into the chamber, methanol, ethanol, and acetone showed an increasing voltage across the standard resistor over a two-hour period. In contrast, carbon dioxide exhibited a decreasing voltage over time. This difference in response suggests distinct interactions between these gases and the sensor material or measurement setup, highlighting the potential for differential

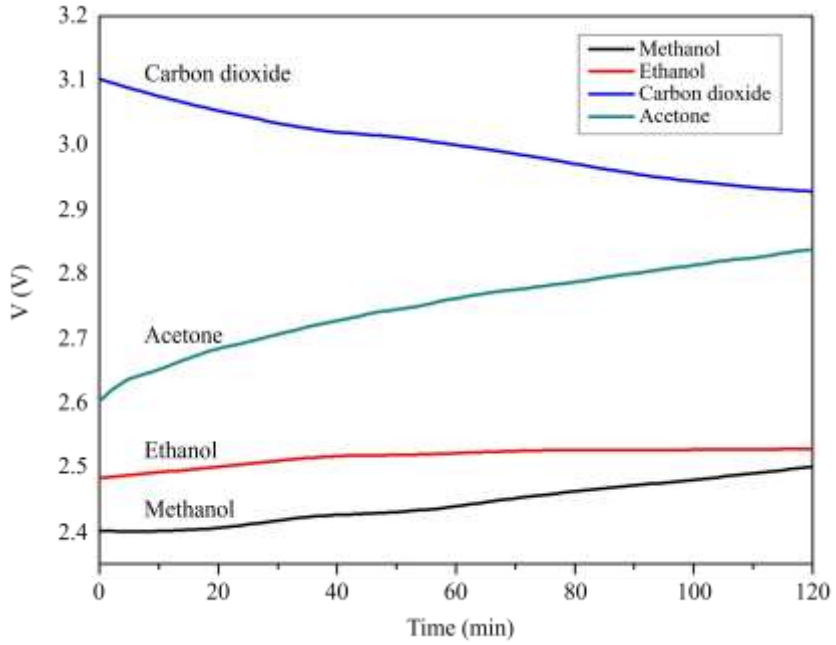

Figure 5. The graph of the Voltage (across standard resistor) vs Time for the carbon films synthesized from banana peel measured in 1000 ppm of methanol, ethanol, carbon dioxide and acetone.

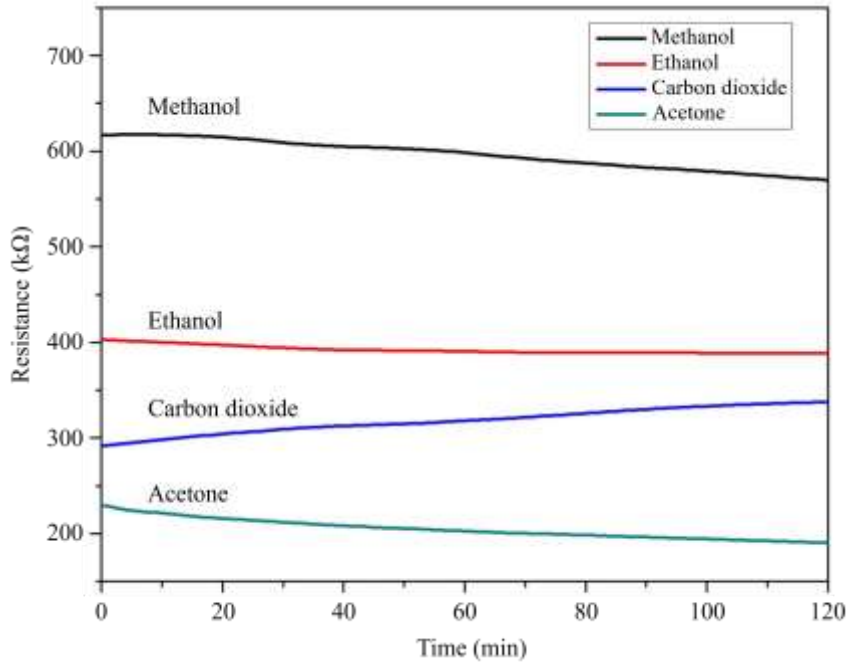

Figure 6. The graph of the Resistance vs Time for the carbon films synthesized from from banana peel measured in 1000 ppm of methanol, ethanol, carbon dioxide and acetone.

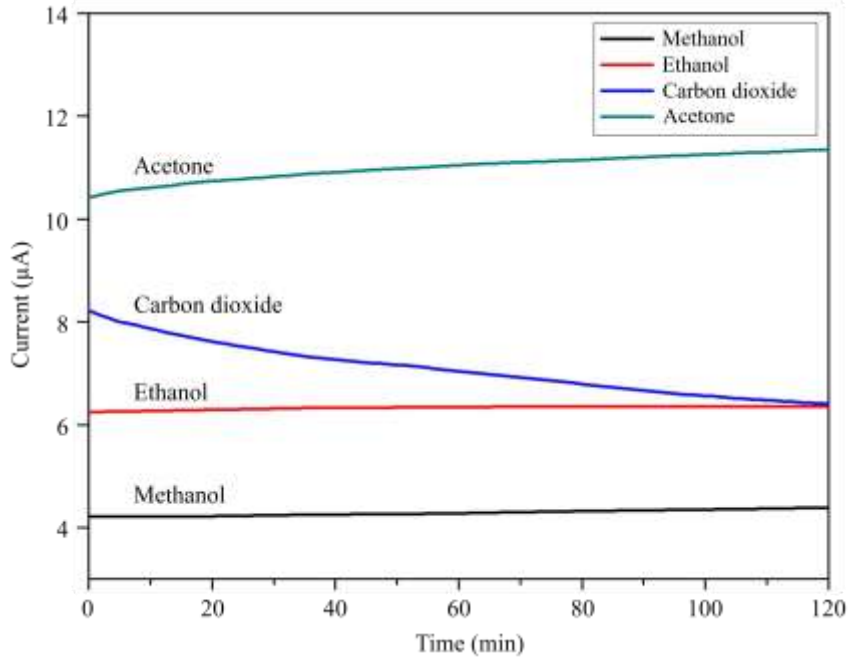

Figure 7. The graph of the Current vs Time for the carbon films synthesized from the banana peel measured in 1000 ppm of methanol, carbon dioxide and acetone.

detection based on the specific gas present. When methanol, ethanol, or acetone gas interacts with the carbon sample, gas denotes electrons into the sample and increases the charge carrier density. Because of this, the conductivity of the sample increases, which means it reduces the resistance of the sample. In this scenario, methanol, ethanol, and acetone act as reducing gases, while carbon dioxide acts as an oxidizing gas. The gas sensitivities are summarized in Table 1.

Table 1. Gas sensitivity of the carbon films synthesized from the banana peels.

Vapor	Gas sensitivity (%)
Methanol	8.35
Ethanol	3.46
Carbon dioxide	16.93
Acetone	17.60

The sheet resistance of the samples synthesized from banana peels was measured as 4.4 kΩ/cm² using the Jandel RM3000+ system. This sheet resistance is significantly less than that of carbon films fabricated using carbon powder derived from rubber wood saw dust and acacia tree branches. The sheet resistance of the carbon films fabricated using carbon powder derived from rubber wood saw dust and acacia tree branches was in MΩ/cm^2 range [6, 15]. Moderate electrical conductivity increased by higher carbonization temperatures render it useful for supercapacitors and batteries.

Containing of oxygen-containing functional groups such as carboxyl, hydroxyl and carbonyl influence adsorption capacity [28]. These groups originate from the raw biomass and are further modified during carbonization and activation processes. The oxygen containing functional groups are as follows. Carboxyl (-COOH) enhances cation exchange capacity, and is crucial for metal adsorption. Hydroxyl (-OH) can be found on the surface, improves water adsorption and interaction with polar molecules. Carbonyl (C=O) presents in aldehydes, ketones, and quinones, influencing redox properties. In addition, lactone (-OCO-) contributes to acidic characteristics and adsorption capacity. Phenolic (-OH on benzene rings) increases surface acidity and ability to interact with metals

and organic pollutants. Nitrogen containing functional groups are Amine (-NH_2, -NHR, -NR_2), Pyridinic Nitrogen (N in a six-membered ring), Pyrrolic Nitrogen (N in a five-membered ring) and Quaternary Nitrogen (N^+ in graphitic layers). Furthermore, sulfur containing oxides are Sulfone (-SO_2-), Thiol (-SH) and Sulfonic Acid (-SO_3H). Alkene (-C=C-) and Alkyl (-CH_3, -CH_2-) are the other functional groups. These functional groups affect surface charge, hydrophilicity, adsorption capacity and catalytic activity.

Bio mass gas sensors can be regenerated via thermal, chemical, or microwave treatment, maintaining efficiency over multiple cycles. Phosphoric acid was used for chemical activation by us. Chemical activation increases specific surface area and functional groups. Because adsorption efficiency depends on solution pH (for aqueous pollutants), our carbon powder was washed using distilled water to control pH value. Biomass-derived carbon has a larger specific surface area as high as 3000 m^2/g in activated forms. The pore structures such as micropores, mesopores and macropores enhances its ability to adsorb gases, heavy metals, and organic pollutants.

Carbon derived from banana peels exhibits unique properties due to the natural composition of the biomass, which contains cellulose, hemicellulose, lignin, and minerals [29]. The properties of this carbon depend on the carbonization temperature, activation process, and treatment conditions. Banana peel carbon has moderate to high surface area, typically 200–1500 m^2/g, depending on activation method. They possess higher porosity when chemically activated using phosphoric acid. Furthermore, they adsorb CO_2, CH_4, and VOCs due to its porous nature. They are stable up to ~600°C under inert conditions. Physisorption is the dominant mechanism for gas adsorption on biomass carbon. It is a reversible process driven by Van der Waals forces. Lower temperatures favor Physisorption. The gas sensitivity of our samples was measured at room temperature. CO_2 is adsorbed due to its small size and high affinity for polar groups. Mostly found functional groups of banana peel derived carbon are Carboxyl (-COOH), hydroxyl (-OH) and carbonyl (C=O).

The highest sensitivity was measured in acetone. Since acetone has a nonpolar character, it interacts well with the nonpolar carbon surface. The π-electrons of aromatic structures in carbon interact with the π-system of acetone [30, 31]. If biomass carbon contains oxygen-containing functional groups (e.g., hydroxyl, carboxyl), they can form hydrogen bonds with acetone's carbonyl group. In addition, Acetone has a dipole moment, which can interact with polar functional groups present on the biomass carbon. If the biomass carbon has charged functional groups (e.g., carboxylates, phenolic groups), they may attract or repel acetone depending on the solution pH. Oxygen-containing groups (-OH, -COOH) can enhance adsorption by forming specific interactions with acetone.

CONCLUSIONS

The sheet resistance of the samples synthesized from banana peels was 4.4 $k\Omega/cm^2$, which is significantly less than that of carbon films grown using carbon powder derived from rubber wood saw dust and acacia tree branches. The SEM images of the samples explore a highly porous structure. The porosity of the film samples was estimated to be 14%, which is prominently responsible for adsorbing vapors and gases. According to the variation of resistance after adsorbing gas or vapor, while acetone, ethanol and methanol behave as a reducing gas, CO_2 gas acts as an oxidizing gas. However, the resistance of the samples did not reach the saturation value within 2 hour duration, because the temporal variation in the electrical resistance of carbon derived from banana peels exhibits a significantly slower rate compared to that of carbon synthesized from acacia tree branches and rubber sawdust. The gas sensitivity of all our samples was measured at the room temperature. Physisorption process dominates at lower temperatures. Van der Waals forces are responsible for the physisorption process. The natural composition of the biomass with cellulose, hemicellulose, lignin, and minerals is the unique property of carbon derived from banana peels. The functional groups of Carboxyl, hydroxyl and carbonyl found in carbon prepared from banana peels are responsible for the adsorption of certain gases and vapors. Dipole moment in acetone interacts with polar functional

groups in the biomass carbon. The average crystallite size of the samples was found to be 1.07 nm, which confirms the amorphous nature of carbon samples.

REFERENCES

1. Tseng RL, Wu FC, Juang RS. Liquid-phase adsorption of dyes and phenols using pinewood-based activated carbons. Carbon 2003; 41(3): 487–95.
2. Malik PK. Dye removal from wastewater using activated carbon developed from sawdust: adsorption equilibrium and kinetics. J Hazard Mater 2004; 113(1–3): 81–8.
3. Tancredi N, Medero N, Moller F, Piriz J, Plada C, Cordero T. Phenol adsorption onto powdered and granular activated carbon, prepared from Eucalyptus wood. J Colloid Interface Sci 2004; 279: 357–63.
4. Akmil-Başar C, Önal Y, Kılıçer T, Eren D. Adsorptions of high concentration malachite green by two activated carbons having different porous structures. J Hazard Mater 2005; 127(1–3): 73–80.
5. Kumar BGP, Miranda LR, Velan M. Adsorption of Bismark Brown dye on activated carbons prepared from rubberwood sawdust (Hevea brasiliensis) using different activation methods. J Hazard Mater 2005; 126(1–3): 63–70.
6. Chathuranga Rathnayake, Karunarathna PGDCK, Dharmasena PASV, Samarasekara P. Synthesis and Characterization of Sustainable, Low-Cost, Biomass- Derived Carbon Films from Hevea Brasiliensis (Rubber) Wood for Environmentally Friendly Gas Sensors with Enhanced Selectivity and Sensitivity to Polar Vapors and Hazardous Gases. Journal of Thin Films Coating Science Technology and Application- STM journals 2025; 12(1): 1-22.
7. Wu FC, Tseng RL. Preparation of highly porous carbon from fir wood by KOH etching and CO2 gasification for adsorption of dyes and phenols from water. J Colloid Interface Sci 2006; 294(1): 21–30.
8. Heidari A, Younesi H, Rashidi A, Ghoreyshi AA. Adsorptive removal of CO2 on highly microporous activated carbons prepared from Eucalyptus camaldulensis wood: effect of chemical activation. J Taiwan Inst Chem Eng 2014; 45: 579–588.
9. Dıaz-D´ ıez MA, Gómez-Serrano V, Fernández González C, Cuerda-Correa EM.´ Macıas- Garc´ ıa A. Porous texture of activated carbons prepared by phosphoric acid´ activation of woods. Appl Surf Sci 2004; 238(1–4): 309–313.
10. Mohanty K, Das D, Biswas MN. Adsorption of phenol from aqueous solutions using activated carbons prepared from Tectona grandis sawdust by ZnCl2 activation. Chem Eng J 2005; 115(1–2): 121–31.
11. Wu FC, Tseng RL, Juang RS. Preparation of highly microporous carbons from fir wood by KOH activation for adsorption of dyes and phenols from water. Sep Purif Technol 2005; 47(1–2): 10–19.
12. Danish M, Hashim R, Ibrahim MNM, Rafatullah M, Ahmad T, Sulaiman O. Characterization of Acacia mangium wood based activated carbons prepared in the presence of basic activating agents. Bioresources 2011; 6(3): 3019–3033.
13. Danish M, Hashim R, Ibrahim MNM, Rafatullah M, Sulaiman O. Surface characterization and comparative adsorption properties of Cr(VI) on pyrolysed adsorbents of Acacia mangium wood and Phoenix dactylifera L. stone carbon. J Anal Appl Pyrol 2012; 97: 19–28.
14. Danish M, Hashim R, Ibrahim MNM, Sulaiman O. Optimization study for preparation of activated carbon from Acacia mangium wood using phosphoric acid. Wood Sci Technol 2014; 48: 1069–1083.
15. Ranasinghe RASR, Rathnathilaka KAC, Karunarathna PGDCK, Samarasekara P. Carbon gas sensors synthesized using acacia auriculiformis tree branches to detect methanol, ethanol, acetone vapors and ammonia gas. Ceylon Journal of Science 2024; 53(2): 207-218.
16. Samarahewa CA, Sunil Dehipawala, Samarasekara P. Optimization of gas sensitivity of CuO/carbon composites with carbon particles synthesized from acacia auriculiformis branches. STM Journals: International Journal of Membranes 2024; 1(1): 22-30.

17. Maharjan J, Jha VK. Activated carbon obtained from banana peels for the removal of As(III) from water" Scientific world 2022; 15(15): 145-157.
18. Erk N, Bouali W, Genc AA, Salamat Q, Soylak M. An ultrasensitive electrochemical sensor using banana peel activated carbon/NiFe2O4 /MnCoFe-LDH nanocomposites for anticancer drug determination. ACS Omega 2024; 9(25): 27446-27457.
19. Al-sareji OJ, Grmasha RA, Meiczinger M, Al-Juboori RA, Somogyi V, Hashim KS. A sustainable banana peel activated carbon for removing pharmaceutical pollutants from different waters: production, characterization, and application. Materials 2024; 17(5): 1032.
20. Gautam M, Patodia T, Gupta V, Sachdev K, Kushwaha HS. Synthesize of high surface area activated carbon from banana peels biomass for zinc-ion hybrid super-capacitor. Journal of energy storage 2024; 102(A): 114088.
21. Nadew TT, Keana M, Sisay T, Getye B, Habtu NG. Synthesize of activated carbon from banana peels for dye removal of an aqueous solution in textile industries: optimization, kinetics, and isotherm aspects. Water Practice & Technology 2023; 18(4): 947-966.
22. Maia LS, Duizit LD., Pinhatio FR, Mulinari DR. Valuation of banana peel waste for producing activated carbon via NaOH and pyrolysis for methylene blue removal. Carbon letters 2021; 31(4): 749-762.
23. Girgis BS, Temerk YM, Gadelrab MM, Abdullah ID. X-ray diffraction patterns of activated carbons prepared under various conditions. Carbon letters 2007; 8: 95-100.
24. Farma R, Wahyuni F, Awitdrus. Physical properties analysis of activated carbon from oil palm empty fruit bunch fiber on methylene blue adsorption. Journal of Technomaterial Physics 2019; 1: 67-73.
25. Tahir D, llyas S, Rahmat R, Heryanto H, Fahri AN, Rahmi MH, Abdullah B, Hong CC, Kang HJ. Enhanced Visible-Light Absorption of Fe_2O_3 Covered by Activated Carbon for Multifunctional Purposes: Tuning the Structural, Electronic, Optical, and Magnetic Properties. ACS Omega 2021; 6(42): 28334-28346.
26. Russo C, Apicella B, Tregrossi A, Ciajolo A, Le KC, Torok S, Bengtsson PE. Optical band gap analysis of soot and organic carbon in premixed ethylene flames: comparison of in-situ and ex-situ absorption measurements. Carbon 2019; 158: 89-96.
27. Yorgun S, Yıldız D. Preparation and characterization of activated carbons from Paulownia wood by chemical activation with H3PO4. J Taiwan Inst Chem Eng 2015; 53:122–131.
28. Kundu C, Biswas S, Thomas BS, Appadoo D, Duan A, Bhattacharya S. Evolution of functional group of lignocellulosic biomass and its delignified form during thermal conversion using synchrotron-based THz and laboratory-based in-situ DRIFT spectroscopy. Fuel 2023; 348: 128579.
29. Salim RM, Asik J, Sarjadi MS. Chemical functional groups of extractives, cellulose and lignin extracted from native Leucaena leucocephala bark. Wood Science and technology 2021; 55: 295-313.
30. Koczorowski T, Rebis T. The Influence of an Extended π Electron System on the Electrochemical Properties and Oxidizing Activity of a Series of Iron(III) Porphyrazines with Bulky Pyrrolyl Substituents. Molecules 2023; 28(20): 7214.
31. Zeng L, Liu X, Chen X, Soutis C. π - π interaction between carbon fibre and epoxy resin for interface improvement in composites. Composites Part B: Engineering 2021; 220: 108983.

